

## Alberta Multiwell Micro-Pilot Testing for CBM Properties, Enhanced Methane Recovery, and CO<sub>2</sub> Storage Potential

Matthew J. Mavor, Tesseract Corporation

William D. Gunter, John R. Robinson, Alberta Research Council

### ABSTRACT

The Alberta Research Council (ARC) is performing a project entitled "Sustainable Development of Coalbed Methane; A Life-Cycle Approach to Production of Fossil Energy" that is funded by an international consortium of companies. The main objectives of the project are to reduce greenhouse gas emissions by subsurface injection of CO<sub>2</sub> into deep coalbeds and to enhance coalbed methane recovery and production rates. We have performed extensive field tests that includes efforts on two wells located near the towns of Fenn and Big Valley in Alberta that penetrated Medicine River (Mannville) coal seams. This paper presents test procedures, quantitative data measured during this effort, and the interpretation thereof. The evaluation was completed over three years ago and was based upon procedures described previously.<sup>1</sup> These data have allowed complete characterization of the coal seam properties with new insights gained into the behavior of coal seams, the volume of natural gas that can be produced, and the volumes of CO<sub>2</sub> that can be sequestered in this area.

The fieldwork began by reentering the Gulf Canada (now ConocoPhillips) well FBV 4A-23-36-20 (FBV 4A) well. We conducted a series of single well micro-pilot tests. We began by production and shut-in testing to obtain estimates of the reservoir pressure and permeability before CO<sub>2</sub> injection. A CO<sub>2</sub> injection test was followed by a shut-in test to insure that CO<sub>2</sub> injection was possible. We then injected over 91,500 m<sup>3</sup> of CO<sub>2</sub> vapor in 12 separate injection cycles. Although CO<sub>2</sub> reduced the absolute permeability, injectivity actually increased. The CO<sub>2</sub> was allowed to soak into the coal and we returned the well to production. Post-injection testing allowed us to determine the CO<sub>2</sub> sweep efficiency as well as the ECBM and CO<sub>2</sub> storage potential. Fourteen months later, we injected 83,500 m<sup>3</sup> of flue gas using underbalanced drilling equipment that was followed by a post injection-production test.

A second well (FBV 5) was drilled 487 m north of the first well. FBV 5 was cored and logged for reservoir property data. The well was then cased and completed in one Medicine River coal seam. A combination of production tests and water-injection falloff tests were conducted to determine original reservoir pressure, permeability, and gas composition. N<sub>2</sub> injectivity tests were performed before injecting 75,483 m<sup>3</sup> of a 53-47 mix of N<sub>2</sub> and CO<sub>2</sub>. The gas mixture was allowed to soak into the coal and the well was returned to production.

All of the post-injection production tests of both wells included detailed measurement of pressure and temperature conditions as well as gas composition variations vs. time. These data allowed us to determine the changes in permeability caused by the injected gas, to estimate possible hydrocarbon sweep efficiency, and possible CO<sub>2</sub> storage volumes.

### FBV 4A MICRO-PILOT TESTING

Gulf Canada donated the FBV 4A well to the project. After review of available data, we concluded that the well penetrated Medicine River coal seams typical of those penetrated by many wells in the Alberta Plains region. The absolute permeability also appeared to be typical.

**FBV 4A History** The FBV 4A well was originally an oil production well but after the original completion was abandoned, the well was recompleted into two Medicine River (Mannville) coal intervals. The upper coal interval was perforated from 1,259 to 1,263 m and the lower coal interval from 1,277 to 1,283 m. A bridge plug set above the lower coal interval isolated the upper interval, which is the subject of this paper.

The upper Mannville coal interval was hydraulically fracture stimulated with a 10 metric ton liquid CO<sub>2</sub> treatment in August 1992. A 40-m<sup>3</sup> liquid CO<sub>2</sub> pre-pad was pumped to initiate the fracture treatment. 160 m<sup>3</sup> of liquid CO<sub>2</sub> was mixed with sand proppant in concentrations increasing from 50 to 200 kg/m<sup>3</sup> and injected into the coal at a rate of 8 m<sup>3</sup>/min at 20 MPa. The fracture gradient was 14.1 kPa/m. The well was produced for 48 hours with a final recorded gas rate of 2,600 m<sup>3</sup>/D. Gas samples taken just before production ceased still contained significant CO<sub>2</sub> concentrations indicating incomplete CO<sub>2</sub> recovery.

A second stimulation treatment was performed in January 1993. 14 m<sup>3</sup> of CO<sub>2</sub> was injected followed by 1,600 m<sup>3</sup> of N<sub>2</sub>. Both fluids were pumped at 1 m<sup>3</sup>/min at a surface pressure of 13 MPa(g).

**Initial Production Testing** We did not have access to the production history of the well until we returned it to production for a short test in March 1998. The well was capable of producing 2,800 m<sup>3</sup>/D against a bottom-hole pressure of approximately 1,400 kPa(g). Water was not produced to surface due to lack of artificial lift.

A static survey and a production / shut-in test with downhole gauges were conducted in June and July 1998. The gas rate during 64 hours of production was constantly declining from 15,900 to 2,970 m<sup>3</sup>/D as artificial lift was not used for the test. Water rates estimated from the rise in water level were roughly constant at 0.92 m<sup>3</sup>/D. Produced gas composition averaged 91.2% C<sub>1</sub>, 1.8% C<sub>2</sub>, 0.3% C<sub>3</sub>, 1.6% CO<sub>2</sub>, and 5.1% N<sub>2</sub>.

Table 1 summarizes the estimates of reservoir properties at that time. Effective permeability to each phase and saturations were estimated from the gas and water rates. San Juan Basin<sup>2</sup> relative permeability data were used since measured data from Mannville coal were unavailable. The data were evaluated with a constant wellbore storage and skin, infinite acting, homogeneous reservoir model<sup>3</sup> using the Kamal and Six coal gas potential relationship.<sup>4</sup>

**Initial CO<sub>2</sub> Injection** We had no previous experience with CO<sub>2</sub> injection into Medicine River coal seams and we planned a single injection test to insure that injection was possible. Bottom-hole transducers were installed and liquid CO<sub>2</sub> was injected at between 100 and 132 liters per min. 21 metric tons (20 m<sup>3</sup>) of liquid CO<sub>2</sub> were displaced into the well. The CO<sub>2</sub> vaporized in the well and an estimated 18 metric tons (17 m<sup>3</sup>) were injected into the coal. CO<sub>2</sub> vapor volume is 542.8 m<sup>3</sup> at standard conditions per m<sup>3</sup> of liquid, therefore 9,230 m<sup>3</sup> of CO<sub>2</sub> vapor were injected into the coal. The final surface injection pressure was 1,500 kPa(g) with a bottom-hole pressure of 10,200 kPa(a). A four-day fall-off test followed injection. Because of the low injection rate, the minimum bottom-hole temperature during injection was 32.8 °C., not greatly reduced from the static temperature of 47.1 °C., and did not affect the transducer.

As all of the injected fluid was in the vapor phase, the falloff period analysis was based on the real gas potential<sup>5</sup> approach. CO<sub>2</sub> vapor properties were computed with equation of state software. Although the data were erratic due to wellbore effects, it was possible to evaluate the data. Injection of CO<sub>2</sub> apparently created or opened existing fractures. The effective permeability to gas estimate (0.632 md) was similar to but slightly greater than the pre-CO<sub>2</sub> estimate of 0.529 md. A skin factor of -4 (equivalent to a fracture half length of 9 m) matched the data.

**Post-CO<sub>2</sub> Production Testing** After the falloff test, FBV 4A was returned to production to determine the effect of the CO<sub>2</sub> upon productivity and reservoir properties. The well stabilized to a tubing head pressure of 160 kPa(g) and a gas rate of 3,200 to 3,300 m<sup>3</sup>/D. 14,635 m<sup>3</sup> of gas were produced over a four-day flow test. This volume was 1.58 times greater than the injected volume of CO<sub>2</sub>. The cumulative CO<sub>2</sub> produced was 4,205 m<sup>3</sup>, 46% of the injection volume.

The first produced gas composition was 100% CO<sub>2</sub> as all gas originated from the well. After 2.2 hours, the gas composition was 55.4% C<sub>1</sub>, 0.8% C<sub>2</sub>, 40.8 CO<sub>2</sub>, and 3.0% N<sub>2</sub>. At the end of the production, the composition was 77.6% C<sub>1</sub>, 1.2% C<sub>2</sub>, 16.6% CO<sub>2</sub>, and 4.7% N<sub>2</sub>.

Analysis of following shut-in period data resulted in essentially the same estimate of absolute permeability (3.47 md) as the estimate obtained from shut-in test data prior to CO<sub>2</sub> injection (3.65 md). The skin factor estimate was 2 indicating that the stimulation caused by CO<sub>2</sub> injection was reversed to the original pre-injection level.

**Extended CO<sub>2</sub> Injection** Once CO<sub>2</sub> injectivity was determined to be sufficient, larger scale CO<sub>2</sub> injection commenced. 180 metric tons of liquid CO<sub>2</sub> were injected during 12 separate injection periods over 31 days. 15 metric tons were injected during each of the 12 injection periods equivalent to 7,750 m<sup>3</sup> of vapor. Injection time ranged from 4 to 7 hours at approximate injection rates of 30 l/min. After 12 injection periods, the total vapor volume displaced into the wellbore was 93,050 m<sup>3</sup> of which 91,500 m<sup>3</sup> were injected into the coal seam. Bottom-hole injection pressures declined from 14,000 to 10,600 kPa(a).

The falloff periods were not designed to obtain reservoir property estimates as no attempt was made to minimize wellbore effects. However, we evaluated each of the falloff periods by history matching the observed pressure changes and derivative behavior with a wellbore storage and skin model.<sup>3</sup>

Table 2 summarizes the analysis results from each of the falloff periods. In general, with some exceptions probably due to analysis problems caused by wellbore effects, the effective permeability to gas decreased with continued injection while the skin factor became progressively more negative. The effective permeability to gas decreased from the pre-injection estimates of 0.53 md to 0.24 after injection of 91,500 m<sup>3</sup> of CO<sub>2</sub>: a decrease by a factor of 2.2. The skin factor decreased from -3.6 after the first injection period to -5.3 after the 12<sup>th</sup> injection period. These skin factors corresponded to an increase in the apparent fracture half-length from 6 to 31 m.

As will be discussed later, we believe that the permeability reduction during the falloff periods was due to swelling of the coal caused by sorption of CO<sub>2</sub>. However, the permeability probably increased during injection. The increase in the effective induced fracture length may have been due to creation of new fractures or due to opening pre-existing fractures induced by the original stimulation as reported previously.<sup>6</sup>

Following the final injection, we allowed the CO<sub>2</sub> to soak in the coal for 39 days. The long soak time reduced transient effects caused by CO<sub>2</sub> sorption and methane expulsion.

**Post-CO<sub>2</sub> Production Testing** Near the end of the soak period, the well was killed with water while circulating CO<sub>2</sub> from the well. We wished to eliminate the volume of CO<sub>2</sub> in the wellbore so that the gas composition data measured after the well was returned to production were representative of the gas contained in the coal natural fracture system. The well was then equipped with a rod pump for artificial lift.

Production rates were dramatically reduced by injection of CO<sub>2</sub>. The gas production rate before CO<sub>2</sub> injection was roughly 3,100 m<sup>3</sup>/D. Gas production rates after CO<sub>2</sub> injection were in the range of 680 to 975 m<sup>3</sup>/D, a decrease of 69 to 78%. Water rates dropped from roughly 0.9 to 0.3 m<sup>3</sup>/D, a reduction of 67%. The similar decrease in gas and water production rates indicated that the CO<sub>2</sub> affected both phases equally due to a decrease in absolute permeability. Had the decrease been due to changes in relative permeability caused by near-well saturation changes, the gas-water rate ratio would have differed.

At the end of the production period, cumulative CO<sub>2</sub> production was 19,564 m<sup>3</sup> or 21% of the 91,500 m<sup>3</sup> injected into the coal seam. The initial produced gas composition at the start of production was 30.5% C<sub>1</sub>, 0.3% C<sub>2</sub>, 68.2% CO<sub>2</sub>, and 0.9% N<sub>2</sub>. As will be discussed later, this composition was used to determine the volume of methane displaced by CO<sub>2</sub> and the potential CO<sub>2</sub> storage volumes. The fraction of CO<sub>2</sub> in the produced stream decreased steadily during production. At the conclusion of production, the produced gas composition was 62.3% C<sub>1</sub>, 1.3% C<sub>2</sub>, 34.0% CO<sub>2</sub>, and 2.5% N<sub>2</sub>.

A final shut-in test was performed and evaluated. The effective permeability to gas was reduced from the value of 0.53 md obtained from pre-CO<sub>2</sub> injection tests to 0.17 md. The ratio of the post- to pre-stimulation effective permeability to gas was 0.32. The ratio between the gas rate after CO<sub>2</sub> injection to the rate before CO<sub>2</sub> injection was identical, 0.32. The corresponding water rate ratio was 0.34. The ratio between the pre- and post-CO<sub>2</sub> absolute permeability was 0.27. The final absolute permeability estimate was 0.985 md. The consistency of the ratios supports that the production decrease was due to absolute permeability reduction.

The reduction in the effective permeability to gas appeared to be uniform. The post-CO<sub>2</sub> skin factor 1.78 was the same as the value of 1.8 obtained from the pre-CO<sub>2</sub> test. This indicates that the near-well absolute permeability reduction was similar to the reduction away from the well.

The estimates of the near-well gas and water saturations after CO<sub>2</sub> injection were very similar to those obtained before injection. This agreement indicated that injection of CO<sub>2</sub> did not displace water away from the wellbore.

**Flue Gas Injection** Fourteen months after the final production period, we injected flue gas into the FBV 4A well. The purposes of the test were to determine injectivity and to conduct a single well micro-pilot test using both CO<sub>2</sub> and N<sub>2</sub>.

The well was returned to production before flue gas injection to obtain gas composition after the extended soak. The gas rate stabilized at approximately 2,400 m<sup>3</sup>/day at a casing pressure of 400 kPa(g). Approximately 3,400 m<sup>3</sup> of gas were produced during the test. The gas rate was substantially greater than the final gas rate of 975 m<sup>3</sup>/D at a surface pressure of roughly 400 kPa(g) recorded after CO<sub>2</sub> injection due to the near-well pressure increase during the extended shut-in.

We used Northland Energy Corporation's flue gas underbalanced drilling system for flue gas injection. The system used propane-fired compressors to generate flue gas. The flue gas was captured, passed through a catalytic converter to remove oxygen, and compressed in four stages with inter-cooling and scrubbing between each stage. A final trap recovered oil from the compressed gas. The flue gas was then injected downhole.

After initial start up problems, flue gas injection continued for six days at a injection rates between 11 and 24 m<sup>3</sup>/min. at a pressure of 12,400 kPa(g). The total amount of flue gas injected was 85,000 m<sup>3</sup>. The volume injected into the reservoir was 83,450 m<sup>3</sup>. Argon was injected as a tracer every 12 hours. 248 m<sup>3</sup> of argon was injected over the six-day injection period. Eight flue gas samples were taken throughout the injection. Injected composition averaged 84.2% N<sub>2</sub>, 12.4% CO<sub>2</sub>, 2.1% Ar, and 1.2% CO.

Following flue gas injection, the 4A well was shut-in to reduce the transient effects of injection. Bottom-hole pressure gauges were left in the well to measure falloff data. The data were analyzed to obtain estimates reservoir properties after flue gas injection. The pressure data indicated composite reservoir model<sup>7</sup> behavior with a near-well region of greater permeability to gas (3.43 md) with a far well region of lesser permeability to gas (1.2 md). Assuming that gas injection did not displace water, the near and far region absolute permeability values were 23.7 and 8.3 md, respectively. The near-well region skin factor was 0.7. Flue gas injection substantially increased the absolute permeability from the 1 md post-CO<sub>2</sub> injection. We believe that this increase was due to stripping CO<sub>2</sub> and methane from the coal matrix causing matrix shrinkage.

Natural fracture permeability varied dramatically throughout the various tests. Figure 1 illustrates the estimated values.

## **FBV 5 EVALUATION AND MICRO-PILOT TESTING**

Gulf Canada at the consortium's recommendation and expense drilled a second well, the Fenn Big Valley 5-23-36-20 (FBV 5) into the Medicine River (Manville) coal seams. This well was located 493 m north of the FBV 4A well. Both wells were completed in the same upper coal interval.

After spudding, a 200-mm hole was drilled to 1,257 m. A 9.1-m core barrel was used to core shale and coal between depths of 1,257 and 1,264.5 m with near 100% recovery. The well was deepened to TD at 1,303 m and logged. Following logging, 139.7-mm casing was run and cemented in place. A casing conveyed pressure / temperature transducer connected to surface with wireline was cemented in the casing-open hole annulus to monitor pressure and temperature inside the casing at 1,240 m.

A core analysis and log interpretation effort fully described the Upper Medicine River coal gas reservoir properties with well documented analysis methods.<sup>8,9</sup> The properties are summarized in Table 3. Table 4 summarizes the dry, ash-free Langmuir isotherm parameters. Figure 2 compares the Langmuir curves and the measured data points. The dry, ash-free values must be converted to in-situ moisture and ash-content before they can be used. Note that it can be very inaccurate to extrapolate isotherm relationships beyond the measurement range.

The untested lower Medicine River coal seam had a thickness of 6.28 m and an average density of 1.350 g/cm<sup>3</sup>. Total Medicine River coal thickness at this location was 10.40 m with an average density of 1.358 g/cm<sup>3</sup>. Total original gas-in-place volume for both seams was 106.3(10<sup>6</sup>) m<sup>3</sup>/km<sup>2</sup> assuming that the gas content vs. inorganic content relationship was the same for both coal seams.

The upper coal seam was completed by perforating followed by hydraulic fracture stimulation. The water-based stimulation consisted of a 65 m<sup>3</sup> pad and 66 m<sup>3</sup> of water containing 20/40 mesh sand at concentrations ramped from 60 to 240 kg/m<sup>3</sup>. The average pump rate was 8.4 m<sup>3</sup>/min. The fracture gradient was 14.36 kg/m. Proppant was tagged with iridium while water was tagged with scandium. Post-stimulation gamma ray logs indicated that the stimulation was contained within the perforated coal seam with some upward growth into the overlying shale.

The well was cleaned out and tubing, wellhead, rod pump, and rods were installed. Production began by pumping. Gas was produced almost immediately indicating that the coal was gas saturated (gas content equal to storage capacity). Gas and water productivity stabilized at 117 and 1.3 m<sup>3</sup>/D, respectively at a bottom-hole pressure of 251 kPa(a). A shut-in test was dominated by storage and two water injection falloff tests were run to determine reservoir pressure and permeability estimates summarized in Table 3. The low productivity was due to the low absolute permeability of 1.2 md, not due to ineffective stimulation, as the skin factor estimate was -3.5 as expected for this type of stimulation.

**N<sub>2</sub> Injection Testing** After water injection-falloff testing, a N<sub>2</sub> injection-falloff test was conducted. An O<sub>2</sub> tracer confirmed that the injected gases entered the coal seam. O<sub>2</sub> chemically reacts with coal and cannot be produced during subsequent production testing if the O<sub>2</sub> entered the coal.<sup>10</sup>

N<sub>2</sub> stimulation equipment was rigged up on the wellhead. A total of 8,300 m<sup>3</sup> of N<sub>2</sub> vapor was pumped down the wellbore at an injection rate of 23 m<sup>3</sup>/min. 6,931 m<sup>3</sup> entered the coal seam. Injection was stopped periodically to inject eight O<sub>2</sub> slugs into the surface lines. Bottom-hole injection pressure at the end of injection was 15,600 kPa(a). The well was shut-in on surface for nine days to perform a falloff test.

Analysis of the injection data indicated that during injection, the absolute permeability reached 13.8 md. The injection ballooned the natural fracture system and substantially increased the permeability. Analysis of the subsequent falloff test was complicated by pressure dependent permeability behavior. A composite model with a greater near-well permeability than the far region was used to match the data. The near and far region effective permeability estimates were 3.9 and 0.14 md, respectively with a near-region skin factor of -0.15. The far region absolute permeability estimates was 8.7 md, which was still influenced by the injection period.

**Post N<sub>2</sub> Injection Production** After the falloff test, FBV 5 was returned to production by pumping the well for 9 days. Gas and water rates after the first day were 562 and 9.3 m<sup>3</sup>/D, respectively, that declined to 116 and 1.6 m<sup>3</sup>/D, respectively. N<sub>2</sub> injection had little but a positive effect upon productivity. The produced gas composition after 1 day was 30% C<sub>1</sub> and 70% N<sub>2</sub>. After nine days, C<sub>1</sub> concentration climbed to 75.2% while N<sub>2</sub> concentration declined to 24.9%. Bottom-hole pressures were in the range of 1,373 to 1,450 kPa(a).

**Simulated Flue Gas Injection** We conducted a simulated flue gas injection micro-pilot test to obtain data to understand reservoir behavior during processed flue gas injection. The test was designed for a mixture consisting of 50% N<sub>2</sub> and 50% CO<sub>2</sub>. 40,911 m<sup>3</sup> of N<sub>2</sub> and 35,938 m<sup>3</sup> of CO<sub>2</sub> vapor were injected during the 67-hour injection period. Of the total gas volume of 76,849 m<sup>3</sup>, 1,369 m<sup>3</sup> remained in the wellbore at the end of injection. The average injection rate was 10.18 m<sup>3</sup>/min for the N<sub>2</sub> and 8.94 m<sup>3</sup>/min for the CO<sub>2</sub>. After injection of approximately 59,000 m<sup>3</sup>, the CO<sub>2</sub> injection rate decreased due to suction pump problems. 170 m<sup>3</sup> of argon was also injected in slugs at 30-minute intervals. The bottom-hole injection pressure increased gradually to 15,660 kPa(a) at a temperature of 43 °C. The injectivity of this test will be discussed later.

A falloff test was conducted when injection ceased. Analysis of these data was complicated by pressure dependent permeability behavior and was performed with a composite reservoir model. The near and far region effective permeability to gas estimates were 5.9 and 0.14 md, respectively. The far region effective gas permeability estimate was a maximum value due to lack of far region derivative stabilization but in line with that estimated after N<sub>2</sub> injection.

**Final Production Testing** A final 26-day production test was conducted to obtain produced gas composition and gas and water production rate data after the simulated flue gas injection. Gas and water rates were stable at the end of production at 173 and 0.74 m<sup>3</sup>/D, respectively at a bottom-hole pressure of 405 kPa(a). Gas productivity was greater than before the micro-pilot tests while the water productivity was less. The initial produced gas composition included 10.8% C<sub>1</sub>, 0.3% C<sub>2</sub>, 557 ppm C<sub>3</sub>, 499 ppm Ar, 33.0% N<sub>2</sub>, and 57.8% CO<sub>2</sub>. At the end of production, the composition was 53.8% C<sub>1</sub>, 1.1% C<sub>2</sub>, 1,774 ppm C<sub>3</sub>, 564 ppm Ar, 25.0% N<sub>2</sub>, and 19.9% CO<sub>2</sub>. Because of the low productivity, only 2.4% of the injected N<sub>2</sub> and 2.6% of the injected CO<sub>2</sub> was produced during this period.

A shut-in test followed the production period. Unfortunately, wellbore storage effects precluded permeability estimates.

## GAS INJECTIVITY

Although the upper Medicine River coal seam produced gas and water at rates commensurate with a 1.2 to 3.6 md natural fracture system, we had few problems injecting water or gases. We obtained substantial data concerning gas injectivity during this project. Gas injectivity is simply defined as the gas injection rate divided by the down-hole pressure differential required to inject the gas

When injecting gas, two competing processes affect both the absolute permeability and the relative permeability to gas as discussed in detail elsewhere.<sup>11</sup> Concisely, pressure strain (strain=change in volume divided by the original volume) balloons natural fractures and increases porosity and absolute permeability during injection while sorption strain tends to swell the coal matrix which reduces natural fracture porosity and absolute permeability. Injection of gas increases fracture porosity, which in turn, reduces water saturation, increasing relative permeability to gas. Sorption strain, caused by adsorption of stronger adsorbing gases than methane, offsets the gain in permeability during injection to a degree dependent upon the relative magnitude of pressure and sorption strain effects. In some cases, injection increases the aperture of natural fractures or reopens induced fractures to such a degree that the near-well region appears stimulated and skin factors become negative.

The ability to inject strongly adsorbing gases while matrix swelling is significant is due to ballooning existing or extending pre-existing fractures away from the wellbore during injection. The increase in injectivity due to ballooning and water saturation reduction overcomes any reduction in injectivity caused by swelling.

**CO<sub>2</sub> Injectivity** Figure 3 illustrates the pressure differential and the injectivity during each of the 12 CO<sub>2</sub> injection periods vs. the cumulative CO<sub>2</sub> injection volume for the FBV 4A well. The pressure differential required for each injection period decreased by roughly 55% over the twelve injection periods from 6,100 kPa to 2,700 kPa. Injectivity increased from 5.5 m<sup>3</sup>/D-kPa for the first injection period to 13.6 m<sup>3</sup>/D-kPa for the final injection period, an increase of 147%. The injectivity for the 11<sup>th</sup> injection period was the greatest as was the injection rate. As discussed later, injectivity may be sensitive to injection rate.

**Injectivity Comparison** Even more surprising than the increased injectivity in the presence of sorption strain was the greater injectivity of CO<sub>2</sub> than other gases in both wells. Figure 4 illustrates a comparison of injectivity vs. total injected fluid volume for each of the tests. In general, N<sub>2</sub> and flue gas injectivity is similar regardless of the injection well. While the FBV 4A flue gas injectivity began at lower levels due to swelling caused by CO<sub>2</sub> sorption, it eventually was greater than the FBV 5 N<sub>2</sub> - CO<sub>2</sub> flue gas injectivity, partially due to the greater absolute permeability at the FBV 4A location. The FBV 5 N<sub>2</sub> injectivity was similar to the N<sub>2</sub> - CO<sub>2</sub> injectivity.

The greater CO<sub>2</sub> injectivity was likely caused by a combination of greater permeability and/or effective fracture length during injection due to ballooning. While a decrease in permeability was observed for the falloff periods after injection ceased, permeability while injecting was greater than during the falloff periods after injection. Unfortunately, we were unable to obtain accurate permeability estimates during injection. Weakening of the coal matrix by CO<sub>2</sub> may have caused greater ballooning of the natural fracture system (resulting in greater permeability during injection) than possible with the other gases.

When comparing two different gases, the injectivity ratio is dependent on the fluid properties if all other factors are equal including the injection time, effective permeability to gas, and skin factor. Eq. 1 defines the injectivity ratio.

$$\frac{i_1}{i_2} = \frac{\mu_2}{\mu_1} \frac{B_{g2}}{B_{g1}} = \frac{\mu_2}{\mu_1} \frac{z_2}{z_1} \quad (1)$$

Table 5 compares the fluid properties at downhole injection conditions of 14,500 kPa(a) and 47 °C.<sup>12</sup> Based upon this comparison, one would expect CO<sub>2</sub> to have the greatest injectivity and N<sub>2</sub> the least. While the observed trends were in agreement with Table 5, the magnitude of the injectivity ratio was not.

One possible explanation for the injectivity differences was the injection rates at bottom-hole conditions. In the FBV 4A well, flue gas bottom-hole injection rates (at bottom-hole temperature and pressure) increased from roughly 20 to 60 m<sup>3</sup>/D. Bottom-hole CO<sub>2</sub> injection rates were substantially greater and ranged from 95 to 217 m<sup>3</sup>/D. At early times, CO<sub>2</sub> injection rates were over three times the flue gas injection rate. The ratio later was less, roughly a factor of 2.4 for the last CO<sub>2</sub> injection rate period. Since the CO<sub>2</sub> rate was greater, a greater portion of the natural fracture system was filled in a given time by CO<sub>2</sub> than by other gases causing the area of the ballooned, higher permeability, region to be larger, increasing injectivity. In addition, the greater viscosity of CO<sub>2</sub> along with swelling would reduce the volume of leak off from ballooned fractures allowing retention of greater energy for extending the ballooned region. The combination of higher rate and viscosity may increase the frictional drag along fracture surfaces causing more fracture surface movement and greater permeability retention due to asperity creation.

One other major difference was that CO<sub>2</sub> was injected in alternating injection-falloff periods. We believe that the alternating sequence improved injectivity and we received a patent for this process.<sup>13</sup> The improved injectivity may have been

the result of coal failure resulting from weakening by CO<sub>2</sub>. The shut-in periods resulted in more weakening that may have been possible without shut-in periods.

## GAS COMPOSITION DATA ANALYSIS

An important part of this project was to use the gas composition data to assist in understanding the enhanced recovery and storage mechanisms. The analysis discussed in this section was based upon material balance of the injection and production volumes and application of extended Langmuir isotherm theory<sup>14</sup> to determine gas storage capacity vs. composition.

**Gas Composition & Storage Capacity Variations** Gas composition in the near-well region of both wells differed substantially at various times due to injection of CO<sub>2</sub>, N<sub>2</sub>, Ar, and flue gas. Figure 5 illustrates the near well gas composition for FBV 5 at various times for three of the principal gas components. Before the first injection, the gas was 94% C<sub>1</sub>, 3% N<sub>2</sub>, and minor components. Injection of N<sub>2</sub> increased the near-well N<sub>2</sub> conc. to 70% and reduced the C<sub>1</sub> conc. to 30%. Production of the well increased the near-well C<sub>1</sub> conc. to 75% while the N<sub>2</sub> conc. was reduced to 25%. Injection of a 53% N<sub>2</sub> - 47% CO<sub>2</sub> mixture increased the near-well CO<sub>2</sub> conc. to 59%, increased the N<sub>2</sub> conc. slightly to 33%, and reduced the C<sub>1</sub> conc. to 8%. After the final production period, the C<sub>1</sub> conc. increased to 53% while the CO<sub>2</sub> conc. dropped to 20%, and the N<sub>2</sub> conc. dropped to the pre-flue gas injection level. Figure 6 illustrates similar data for FBV 4A.

Extended Langmuir isotherm theory and the isotherm data included in Table 4 allowed computation of the storage capacity of each component and the total storage capacity. Figures 7 and 8 illustrate the estimated storage capacity for each component and the total storage capacity for both wells. The storage capacity values of the individual components do not always sum to the total storativity in Figures 7 and 8 due to the presence of small amounts of ethane and propane included in the calculations.

At the FBV 5 location, injection of N<sub>2</sub> decreased the total storage capacity from 7.6 to 4.9 scc/g due to the lower sorptive capability of N<sub>2</sub>. Production of some of the N<sub>2</sub> increased the near-well storage capacity to 6.7 scc/g. Injection of simulated flue gas increased the total storage capacity to 16.8 scc/g due to the greater affinity for CO<sub>2</sub>. The final production period did not remove all of the CO<sub>2</sub> and as a result, the total storage capacity remained greater than the initial storage capacity.

At the FBV 4A location, injection of CO<sub>2</sub> increased the total storage capacity from 7.57 to 17.06 scc/g due to greater CO<sub>2</sub> sorption. Production of 21% of the CO<sub>2</sub> injection volume reduced the storage capacity to 13.70 scc/g. During the fourteen-month shut-in period, migration of CO<sub>2</sub> away from the near-well region reduced the storage capacity to 12.92 scc/g. Injection of flue gas and the final production period reduced the total storage capacity to 11.02 and 10.50 scc/g, respectively.

**Hydrocarbon Sweep Efficiency & Displacement** We used two primary terms to evaluate hydrocarbon displacement by injected gas. The first term, hydrocarbon displacement efficiency, was the fraction of hydrocarbons removed from an area contacted by an injected fluid. The second term, hydrocarbon displacement ratio was the ratio of the displaced hydrocarbon volume to the injected fluid volume.

The hydrocarbon displacement efficiency,  $E_{dh}$ , was computed from the ratio of the end to the beginning hydrocarbon storage capacity with Eq. 2. The area containing the injected fluid volume,  $A_d$ , was computed with Eq. 3 based upon the storage capacity of the injected fluid. The volume of hydrocarbons displaced from the displacement area,  $D_h$ , was computed with Eq. 4 based upon the change in the hydrocarbon storage capacity. Finally, the hydrocarbon displacement ratio,  $R_d$ , was computed with Eq. 5.

$$E_{dh} = 1 - \frac{G_{sh2}}{G_{sh1}} \quad (2) \quad A_d = \frac{V_i}{h\bar{\rho}_c G_{si}} \quad (3) \quad D_h = A_d h \bar{\rho}_c (G_{sh1} - G_{sh2}) \quad (4) \quad R_d = \frac{D_h}{V_i} \quad (5)$$

Estimates of hydrocarbon displacement efficiency were computed from the storage capacity information illustrated in Figures 7 and 8. As an example, at the FBV 5 location, before injection of N<sub>2</sub>, the hydrocarbon storage capacity was 7.43 scc/g. After injection of a relatively small volume of N<sub>2</sub>, the hydrocarbon storage capacity was reduced to 3.48 scc/g. Therefore, the hydrocarbon displacement efficiency was 53% in the region contacted by N<sub>2</sub>. The N<sub>2</sub> storage capacity after injection was 1.386 scc/g. Since the injected volume was 6,931 m<sup>3</sup>, the displacement area was 878.5 m<sup>2</sup> for a thickness of 3.97 m and an average density of 1.434 g/cm<sup>3</sup>. The hydrocarbon displacement volume in this area was 19,763 m<sup>3</sup>. The ratio of the hydrocarbon displacement volume to the injected fluid volume was 2.85. All gas volumes are at standard conditions since gas storage capacity is at standard conditions. Computations such as these were performed after injection periods and after the production periods that followed injection. Material balance was required to account for all injected and produced volumes.

**Injected Gas Distributions** To evaluate the fluid distributions, we considered the near-well free gas concentration to be uniform within the region contacted by the injected gas. We will discuss the consequences of this simple assumption later. We assumed that the entire thickness adsorbed the gas to convert volume to area estimates. For illustration, we assumed that the gases were distributed elliptically around the wellbore however; the area is the same regardless of the assumed shape.

Figure 9 illustrates the areas required to store the injected fluid volumes at four different times around the FBV 5 well. We discussed the computations above after N<sub>2</sub> was first injected. The second time was after production of 13.9% of the injected N<sub>2</sub> volume. N<sub>2</sub> concentration in the produced gas dropped from 70 to 25%. The produced N<sub>2</sub> volume alone could not explain this reduction. The area required to store the remaining N<sub>2</sub> volume (5,966 m<sup>3</sup>) was 2,909 m<sup>2</sup>. N<sub>2</sub> appeared to move farther away from the well during production although the pressure gradient was toward the well. Physically, sorbed gas was moving away from the well via diffusion through the coal matrix while vapor phase production was toward the well in the coal natural fracture system.

Mixed gas injection ended up with three concentric regions around FBV 5. The near-well region contained all of the CO<sub>2</sub>, some N<sub>2</sub>, Ar, and remaining hydrocarbons. Beyond the near-well region, there was a ring of gases that contained the injected gases not sorbed in the near-well region and the hydrocarbons displaced from the near-well well region. Finally, there was an outer region that contained the displaced hydrocarbons that originated from both the near-well and outer-ring regions and the original hydrocarbon gases.

Mixed gas injection of 75,480 m<sup>3</sup> of 53% N<sub>2</sub> (40,184 m<sup>3</sup>) and 47% CO<sub>2</sub> (35,299 m<sup>3</sup>) displaced 93% of the hydrocarbons from the region contacted by CO<sub>2</sub>. The area required to store the CO<sub>2</sub> volume was 387 m<sup>2</sup>. The hydrocarbon volume displaced from this region by the CO<sub>2</sub> was 12,924 m<sup>3</sup>. The hydrocarbon displacement ratio for the near-well region was 0.366. This value was substantially lower than for N<sub>2</sub> since CO<sub>2</sub>, being more strongly sorbed, contacts much less of the reservoir although the displacement efficiency was substantially greater than for N<sub>2</sub>.

The outer ring region contained 75.6% N<sub>2</sub>, 24.3% hydrocarbons, and Ar in the free-gas phase. The area of this ring was 4,510 m<sup>2</sup> excluding the near-well region. The volume of hydrocarbons displaced from the outer-ring was 124,900 m<sup>3</sup>. This corresponded to a hydrocarbon displacement ratio of 3.1, similar to that for pure N<sub>2</sub> injection. Hydrocarbon displacement by the simulated flue gas injection was 140,200 m<sup>3</sup>. The hydrocarbon displacement ratio was 1.86, intermediate to the results for pure CO<sub>2</sub> and N<sub>2</sub>.

The final computation was for the gas composition after production of the injected N<sub>2</sub>-CO<sub>2</sub> mixture. As for production after pure N<sub>2</sub> injection, the area of the reservoir appeared to increase. The calculated area required to store the remaining CO<sub>2</sub> volume increased by 124% to 866 m<sup>2</sup>. The area required to store the remaining N<sub>2</sub> volume increased by 436% to 26,229 m<sup>2</sup>. This difference will be discussed later.

The same analysis was performed for the FBV 4A well. The upper ellipse in Figure 10 illustrates the area that could contain the CO<sub>2</sub> volumes at three different times, after CO<sub>2</sub> injection, after the subsequent production test, and after the fourteen-month shut-in period. The lower two ellipses illustrate the distribution after the flue gas injection test and after the final production period.

After the first CO<sub>2</sub> injection, the hydrocarbon displacement efficiency was 80.6% within the region contacted by CO<sub>2</sub>, which was less than after N<sub>2</sub> and CO<sub>2</sub> injection in FBV 5. The area containing CO<sub>2</sub> was 1,029 m<sup>2</sup>. The volume of hydrocarbons displaced was 35,119 m<sup>3</sup> corresponding to a hydrocarbon displacement ratio of 0.384.

Following production, the area of containing CO<sub>2</sub> appeared to expand 19% to 1,226 m<sup>2</sup>. After 14 months, the area expanded another 14% to 1,402 m<sup>2</sup>. The degree of expansion was less than for the combination of CO<sub>2</sub> and N<sub>2</sub> due to the stronger sorption properties of CO<sub>2</sub>.

During the flue gas test, the injected volume included 70,289 m<sup>3</sup> of N<sub>2</sub>, 10,367 m<sup>3</sup> of CO<sub>2</sub> and 243 m<sup>3</sup> of Ar. 79,475 m<sup>3</sup> of CO<sub>2</sub> remained in the reservoir after both tests. The CO<sub>2</sub> volume was contained in an area of 1,968.1 m<sup>2</sup>. The hydrocarbon displacement efficiency in this region was 0.552 as production after the 1<sup>st</sup> CO<sub>2</sub> injection and N<sub>2</sub> injection stripped both hydrocarbons and CO<sub>2</sub> from the near well region. The displaced hydrocarbon volume from this region was 10,139 m<sup>3</sup>. The hydrocarbon displacement injection volume ratio was 1.02.

The outer ring region contained 87.1% N<sub>2</sub>, 12.6% hydrocarbons, and 0.4% Ar in the free gas phase resulting in a N<sub>2</sub> storage capacity of 2.01 scc/g. The hydrocarbon displacement efficiency was 0.772. The area of the outer ring region was 22,180 m<sup>2</sup>. The hydrocarbon volume displaced from the outer ring was 200,800 m<sup>3</sup> corresponding to a hydrocarbon displacement ratio of 2.86. The total hydrocarbon displacement ratio to the total injected fluid volume was 2.61. This ratio was higher than for the FBV 5 since the previous CO<sub>2</sub> injection and N<sub>2</sub> forced the CO<sub>2</sub> injected with the flue gas to contact a greater area of the reservoir.

After the final post-flue gas production period, 71,294 m<sup>3</sup> of CO<sub>2</sub> remained in the reservoir within an area of 2,950 m<sup>2</sup>. The area of the outer ring appeared to expand to 30,130 m<sup>2</sup>.

**Distribution Errors** We used the analysis of the gas composition data to assist with understanding the variation in produced gas composition data. There were two primary assumptions. These were that the gases in the vapor and sorbed phases were in equilibrium and that the gas compositions were constant within a displacement area. There are problems with these assumptions that will cause errors in the estimates of the extent of displacement areas.

After injection of various gases, we shut in the wells and allowed the gases to “soak” in the reservoir. We used this procedure to allow the gas compositions to reach equilibrium. The soak duration varied from 7 to 39 days. Sorption time (which is related to the inverse of diffusivity) is the time required to release 63% of gas stored by sorption. The methane sorption time of the Medicine River coal was 4.9 hours and we believed that seven or more days were sufficient to reach

equilibrium. Application of extended Langmuir isotherm theory requires equilibrium conditions and as a result, we believed that our interpretations of the produced gas composition data immediately after a soak period were reasonable. If there was a sorbed gas composition gradient present, our assumption of uniform concentration distribution underestimated the sorbed region area after a soak period.

Interpretation of the gas composition data at the end of a production period was much more subject to error as the reservoir was not in an equilibrium state. Gas compositions changed rapidly during production. The drop in pressure near the well released methane and CO<sub>2</sub> from the near well region. Due to the low natural fracture porosity, production affected the region beyond the displacement area bringing hydrocarbons back into the displacement region. There was a substantial variation in the gas composition in the natural fracture system through the reservoir. It was likely that diffusion of different gas components in different directions (i.e., into and out of) the coal matrix was occurring simultaneously. These concentration variations may be the reason that the displacement area appeared to be increasing after production. We were less concerned about these errors as we were more interested in using the equilibrium gas composition data to predict hydrocarbon sweep efficiency during a long-term displacement processes.

## **ENHANCED CH<sub>4</sub> PRODUCTION - CO<sub>2</sub> STORAGE POTENTIAL**

One of the primary goals of this project was to predict the volumes of methane that may be produced and the volumes of CO<sub>2</sub> that may be stored under a full-scale ECBM-storage project. We were able to make these computations based upon the data reported in this paper.

Since CO<sub>2</sub> is strongly sorbed, there is a relatively distinct displacement front within the coal seams at the CO<sub>2</sub> - original gas boundary similar to that observed during water flooding with favorable mobility ratios. Under favorable conditions, i.e., uniform permeability, we expect to sweep 70% of a five-spot pattern at breakthrough based upon water flooding studies.<sup>15</sup> Within the CO<sub>2</sub> swept zone, 80.6% of the hydrocarbon gases were displaced by CO<sub>2</sub>. Therefore, we expect to recover up to 56.4% of the hydrocarbons in place at CO<sub>2</sub> breakthrough if the reservoir pressure is maintained relatively constant. Greater recovery would be achieved with a reduction in reservoir pressure.

We estimated maximum primary production potential using a coal gas reservoir simulator for a hypothetical well penetrating a reservoir with an absolute permeability of 4 md, which was slightly greater than that estimated for the upper Medicine River coal seam at the FBV 4A location. Under primary recovery at the FBV 4A site with a 0.32-km<sup>2</sup> (80-acre) development scenario, a properly stimulated well was capable of recovering 43% of the gas-in-place volume over a 6.2 year period if the bottom-hole pressure was maintained at 276 kPa(a) until gas production declined to 1,420 m<sup>3</sup>/D.

Injection of CO<sub>2</sub> at a rate twice the production rate raised the recovery to 56.4% and reduced the recovery time to 3.6 years. Therefore, the incremental gain in recovery was 13.2% of the gas-in-place volume with an economic assist due to the faster recovery.

Total original gas-in-place volume for both seams was 106.3 (10<sup>6</sup>) m<sup>3</sup>/km<sup>2</sup>. Under primary recovery, 45.7 (10<sup>6</sup>) m<sup>3</sup>/km<sup>2</sup> was recovered. The incremental gain in recovery during CO<sub>2</sub> injection was 14.0 (10<sup>6</sup>) m<sup>3</sup>/km<sup>2</sup>.

The gain in recovery due to enhanced recovery could be much greater for a lower permeability reservoir since primary recovery volumes would be low. Economic recovery of gas under primary depletion is not possible for a one-md reservoir such as penetrated by FBV 5. Without regard for cost, the simulated gas recovery factor from a one-md reservoir was 21.7% in 6.4 years. If recovery can be improved to the same level as primary depletion from a four-md reservoir by enhanced recovery, economic operation of production wells may be possible.

The maximum CO<sub>2</sub> storage possible at the time of CO<sub>2</sub> breakthrough was 70% of the pattern area times the CO<sub>2</sub> sorptive capacity. In the swept zone, the CO<sub>2</sub> sorptive capacity was 15.61 scc/g. Therefore, the maximum storage capacity was 10.93 scc/g. Including both Medicine River coal seams, the maximum storage capacity was 154.3 (10<sup>6</sup>) m<sup>3</sup>/km<sup>2</sup>. This volume was equivalent to 286,600 kg tons/km<sup>2</sup>. This estimate assumed that reservoir pressure was maintained at 7,900 kPa(a). Greater CO<sub>2</sub> storage would have resulted if production ceased at breakthrough and CO<sub>2</sub> injection continued, increasing reservoir pressure above the initial level.

## **SUMMARY**

We conducted an extensive testing program on two wells completed in Medicine River Coal seams in the Alberta Plains Region. By sequential injection, soak, and production tests, along with accurate bottom-hole pressure and produced gas composition monitoring, we were able to increase our understanding of the enhanced coalbed methane - CO<sub>2</sub> storage process. The detailed data resulted in conclusions that were opposite to general beliefs before the project started.

It was generally thought that CO<sub>2</sub> injection would be hindered by coal swelling caused by CO<sub>2</sub> sorption. We found the opposite to be the case as CO<sub>2</sub> injectivity was greater than for weakly adsorbing N<sub>2</sub> through the use of alternating injection shut-in sequences and perhaps as the result of coal weakening.

It was generally thought that any injection into a coal seam with one md permeability would be difficult. We found that injection increased the absolute permeability and effective permeability to gas to a level easily allowing injection.



The combination of these two observations suggests that low permeability coal seams that may not be commercial under primary production could still be CO<sub>2</sub> storage sites with the added benefit of improving the possibility for commercial gas productivity.

It was generally thought that CO<sub>2</sub> would displace all of the hydrocarbons away from injection wells. This was not the case as 20% of the hydrocarbons remained in the CO<sub>2</sub> contact area.

We have also found the data to be very useful to investigators that are developing reservoir simulation software to model primary and enhanced recovery from coal seams. These data can serve as history matching files to test the accuracy of the modeling methods.

## ACKNOWLEDGEMENTS

The data from Alberta Canada were collected as part of an Alberta Research Council (ARC) project entitled *Sustainable Development of Coalbed Methane, A Life-Cycle Approach to Production of Fossil Energy*. A consortium of international companies funded this project, which included development of the field procedures and analyses presented in this paper. We gratefully acknowledge the consortium's support and permission to release this paper. Numerous other individuals were involved in the drilling, coring, logging, core analysis, production, and testing operations. We appreciate their contributions to the acquisition of this high quality data set.

## NOMENCLATURE

$A_d$	displacement (contacted) area, $m^2$
$B_{g1}, B_{g2}$	formation volume factor of gas one or two at downhole conditions, reservoir volume/surface volume
$D_h$	hydrocarbon displacement efficiency, dimensionless
$E_{dh}$	hydrocarbon displacement efficiency, dimensionless
$G_{sh2}$	final hydrocarbon storage capacity, scc/g
$G_{sh1}$	initial hydrocarbon storage capacity, scc/g
$G_{si}$	injected fluid storage capacity, scc/g
$h$	reservoir thickness, m
$i_1, i_2$	injectivity of gas one or two, $m^3/D\text{-kPa}$
$R_d$	hydrocarbon displacement ratio, dimensionless
$V_i$	injection volume, $m^3$
$z_1, z_2$	real gas deviation factor of gas one or two at downhole conditions, dimensionless
$\mu_1, \mu_2$	viscosity of gas one or two at downhole conditions, Pa-s
$\bar{\rho}_c$	average reservoir (coal) density, $g/cm^3$

## References

1. Mavor, M.J., Gunter, W.D., Robinson, J.R., Law, D., H-S, and Gale, J.: "Testing for CO<sub>2</sub> Sequestration and Enhanced Methane Production from Coal," paper SPE 75683, SPE Gas Tech. Sym., Calgary, Alberta, Canada (April 3 - May 2, 2002).
2. Gash, B.W.: Voltz, R.F., Potter, G., and Corgan, J.M.: "The Effects of Cleat Orientation and Confining Pressure on Cleat Porosity, Permeability, and Relative Permeability," Paper 9321, *Proceedings of the 1993 International Coalbed Methane Symposium*, Vol. 1, University of Alabama/Tuscaloosa (May 17-21, 1993) pp. 247-255.
3. Agarwal, R.G., Al-Hussainy, R. and Ramey, H.J., Jr.: "An Investigation of Wellbore Storage and Skin Effect in Unsteady Liquid Flow: I. Analytical Treatment," *Society of Petroleum Engineers Journal* (Sept. 1970) pp. 279-290.
4. Kamal, M.M. and Six, J.L.: "Pressure Transient Testing of Methane Producing Coalbeds," paper SPE 19789, 64th Annual Tech. Conference and Exhibition of the Society of Pet. Eng., San Antonio, Texas (October 8-11, 1989).
5. Al-Hussainy, and H.J. Ramey, Jr.: "Application of Real Gas Flow Theory to Well Testing and Deliverability Forecasting," *Journal of Petroleum Technology*, (May 1966) pp. 637-642.
6. Fokker, P.A. and van der Meer, L.G.H.: "The Injectivity of Coalbed CO<sub>2</sub> Injection Wells," Gale, J. and Kaya, Y. (eds): *Proceedings of the 6<sup>th</sup> International Conference on Greenhouse Gas Control Technologies*, Vol. I, Elsevier Science, Ltd. Oxford, UK (2003) pp. 551-556.
7. Satman, A.: "Pressure Transient Analysis of a Composite Naturally Fractured Reservoir," paper SPE 18587, Society of Petroleum Engineers (1991).
8. Mavor, M.J.: "Coalbed Methane Reservoir Properties" in *A Guide to Coalbed Methane Reservoir Engineering*, Saulsberry, J.L., Schafer, P.S., and Schraufnagel, R.A. (Editors), Gas Research Institute Report GRI-94/0397, Chicago, Illinois (March 1996).
9. Mavor, M.J. and Nelson, C.R.: *Coalbed Reservoir Gas-In-Place Analysis*, Gas Research Institute Report No. GRI-97/0263, Chicago, Illinois (October 1997).

10. Puri, R., Voltz, R., and Duhrkopf, D.: "A Micro-Pilot Approach to Coalbed Methane Reservoir Assessment," Paper 9556, *Intergas '95 Proceedings*, University of Alabama / Tuscaloosa, Tuscaloosa, Alabama (May 15-19, 1995) pp. 265-274.
11. Mavor, M.J. and Gunter, W.D.: "Secondary Porosity and Permeability of Coal vs. Gas Composition and Pressure," SPE publication pending (2004).
12. Huber, M.L.: *NIST Thermophysical Properties of Hydrocarbon Mixtures Database – SUPERTRAPP, Version 3.0, Users' Guide*, National Institute of Standards and Technology, Gaithersburg, MD (September 1999).
13. Gunter, W.D., Mavor, M.J., and Law, D.H-S: *Process for Recovering Methane and/or Sequestering Fluids*, United States Patent 6,412,559 (July 2, 2002).
14. Yang, R.T.: *Gas Separation by Adsorption Processes*, Imperial College Press, London, (1997) pp. 49-51.
15. Lake, L.W.: *Enhanced Oil Recovery*, Prentice Hall, New Jersey (1989) p. 191.

**Table 1. FBV 4A Properties Before CO<sub>2</sub> Injection**

Property	Units	Value
Original pressure (12/17/92)	kPa	7,901
Average pressure (7/2/98)	kPa	7,653-7,770
Pressure gradient to surface	kPa/m	6.11
Pressure depth below ground	m	1,252.54
Absolute permeability	md	3.65
Near-well gas saturation	%	40
Near-well water saturation	%	60
Effective permeability to gas	md	0.529
Effective permeability to water	md	0.157
Relative permeability to gas	-	0.145
Relative permeability to water	-	0.157
Skin factor	-	1.8
Wellbore storage coefficient	m <sup>3</sup> /kPa	8.6(10 <sup>-5</sup> )
Radius of investigation	m	63

**Table 2. FBV 4A CO<sub>2</sub> Falloff Period Properties**

Shut-In Period	Shut-in Duration	Effective Perm. to Gas	Skin Factor	Apparent Fracture Length
	hours	md	--	m
Pre-Injection-		0.53	1.8	-
1	41.37	0.40	-3.6	6.0
2	42.19	0.50	-4.2	11.0
3	42.89	0.50	-4.2	11.0
4	42.97	0.40	-4.2	11.0
5	44.31	0.55	-4.3	12.1
6	40.26	0.51	-4.3	12.1
7	42.31	0.52	-4.3	12.1
8	42.42	0.40	-4.7	18.1
9	41.08	0.41	-4.7	18.1
10	42.75	0.30	-5.1	27.0
11	44.34	0.30	-5.4	36.4
12	145.55	0.24	-5.3	31.4

**Table 3. FBV 5 Upper Medicine River Coal Properties**

Property	Units	Value	Units	Value
<i>Geometry</i>				
Upper Medicine River Coal Top Depth	meters	1,257.5	feet	4,125.7
Upper Medicine River Coal Bottom Depth	meters	1,262.0	feet	4,140.4
Upper Medicine River Coal Thickness	meters	3.97	feet	13.0
<i>Reservoir Temperature, Pressure, Permeability, and Saturations</i>				
Average Temperature	°C.	47.2	°F.	117
Average Pressure	kPa(a)	7,901	psia	1,146
Effective Permeability to Water	$\mu\text{m}^2$	$7.43(10^{-4})$	md	0.753
Effective Permeability to Gas	$\mu\text{m}^2$	$1.9(10^{-5})$	md	0.019
Absolute Permeability	$\mu\text{m}^2$	$1.16(10^{-4})$	md	1.18
Water Saturation	%	90.9	%	90.9
Gas Saturation	%	9.1	%	9.1
<i>Coal Properties</i>				
Average In-Situ Moisture Content	wt. %	6.72	wt. %	6.72
Average In-Situ Ash Content (moist)	wt. %	15.6	wt. %	15.6
Average In-Situ Density (moist with ash)	$\text{g}/\text{cm}^3$	1.434	$\text{g}/\text{cm}^3$	1.434
Average Sulfur Content (moist)	wt. %	2.99	wt. %	2.99
Organic Fraction Density (dry)	$\text{g}/\text{cm}^3$	1.328	$\text{g}/\text{cm}^3$	1.328
Inorganic Fraction Density (dry)	$\text{g}/\text{cm}^3$	3.081	$\text{g}/\text{cm}^3$	3.081
ASTM Coal Rank Classification	-	hvbB	-	hvbB
Calorific Value (moist, mineral-matter-free)	MJ/kg	30.5	BTU/lbm	13,100
Vitrinite Reflectance	%	0.51	%	0.51
Vitrinite Content (mineral-matter-free)	vol. %	62.8	vol. %	62.8
Inertinite Content (mineral-matter-free)	vol. %	35.8	vol. %	35.8
Liptinite Content (mineral-matter-free)	vol. %	1.4	vol. %	1.4
<i>Gas Content, Composition, and Sorption Time</i>				
In-Situ Sorbed Gas Content (moist with ash)	scc/g	7.57	scf/ton	243
In-Situ Gas Storage Capacity (moist with ash)	scc/g	7.57	scf/ton	243
In-Situ Gas-in-Place/Area	$\text{Mm}^3/\text{km}^2$	43.1	Bscf/mi <sup>2</sup>	3.94
Free Gas Methane Concentration	mole %	94.42	mole %	94.42
Free Gas Ethane Concentration	mole %	1.53	mole %	1.53
Free Gas Propane+ Concentration	mole %	0.29	mole %	0.29
Free Gas Nitrogen Concentration	mole %	3.46	mole %	3.46
Free Gas Carbon Dioxide Concentration	mole %	0.26	mole %	0.26
Coal Sorption Time	hours	4.93	hours	4.93

**Table 4. Upper Medicine River Sorption Properties**

Property	Units	Value	Units	Value
DAF Methane Langmuir Storage Capacity	scc/g	15.14	scf/ton	485.0
Methane Langmuir Pressure	kPa(a)	4,688.5	psia	680.0
DAF Ethane Langmuir Storage Capacity	scc/g	14.15	scf/ton	453.2
Ethane Langmuir Pressure	kPa(a)	1,496.9	psia	217.1
DAF Argon Langmuir Storage Capacity	scc/g	18.53	scf/ton	593.6
Argon Langmuir Pressure	kPa(a)	9,673.4	psia	1,401
DAF CO <sub>2</sub> Langmuir Storage Capacity	scc/g	31.02	scf/ton	993.8
CO <sub>2</sub> Langmuir Pressure	kPa(a)	1,903.0	psia	276.0
DAF Nitrogen Storage Capacity	scc/g	15.01	scf/ton	480.9
Nitrogen Langmuir Pressure	kPa(a)	27,241	psia	3,951
DAF H <sub>2</sub> S Storage Capacity	scc/g	37.82	scf/ton	1,211
H <sub>2</sub> S Langmuir Pressure	kPa(a)	190.0	psia	27.55
DAF H <sub>2</sub> Storage Capacity	scc/g	1.03	scf/ton	33.0
H <sub>2</sub> Langmuir Pressure	kPa(a)	410	psia	59.46

DAF: dry, ash-free - scc:  $\text{cm}^3$  at standard conditions of 101.3 kPa(a) and 15.56 °C

**Table 5. Gas Properties at Injection Conditions**

Fluid	Viscosity	Formation Volume Factor	z Factor	CO <sub>2</sub> /Fluid Injectivity Ratio
	cp	res. vol./surf. vol.	-	-
CO <sub>2</sub>	0.06114	0.02770	0.3370	1.00
N <sub>2</sub>	0.02273	0.08135	1.0481	1.16
13%CO <sub>2</sub> -87%N <sub>2</sub>	0.02315	0.07864	1.0086	1.13
50%CO <sub>2</sub> -50% N <sub>2</sub>	0.02447	0.06740	0.8509	1.01
CH <sub>4</sub>	0.01644	0.06930	0.8764	0.70

Figure 1. FBV 4A Permeability Estimates

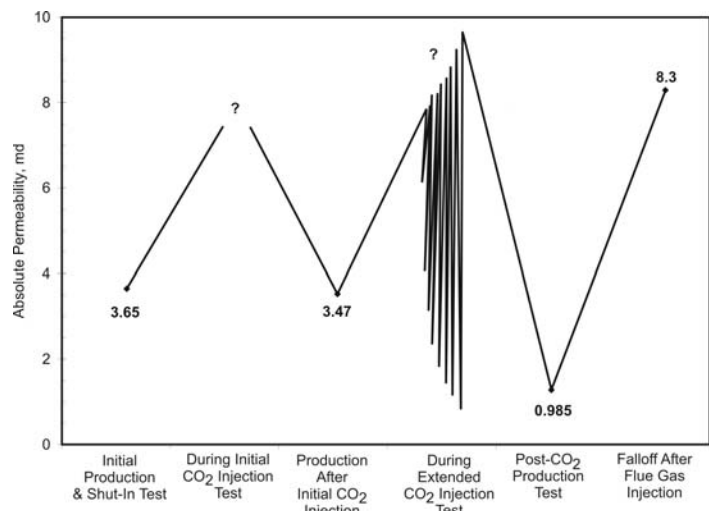


Figure 2. Upper Medicine River Coal Isotherm Data

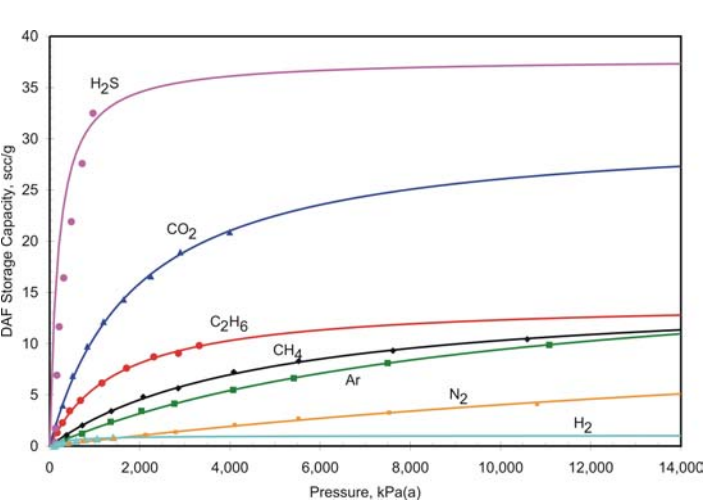


Figure 3. FBV 4A CO2 Injectivity

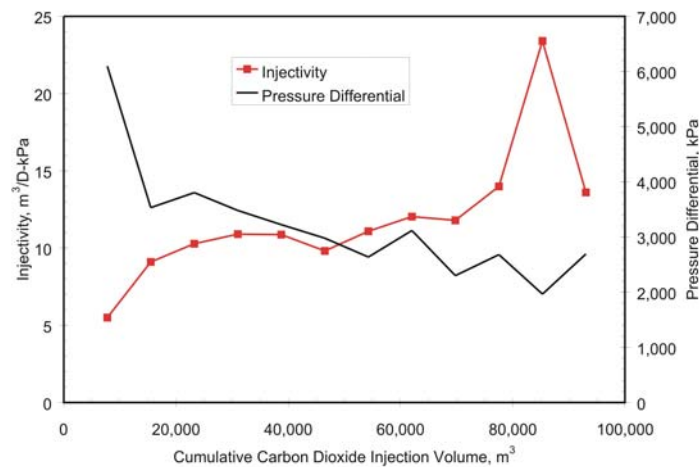


Figure 4. Injectivity Comparison

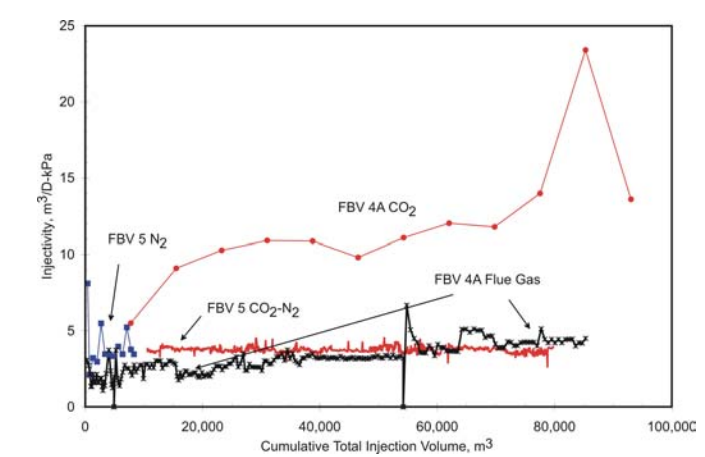


Figure 5. FBV 5 Free Gas Composition

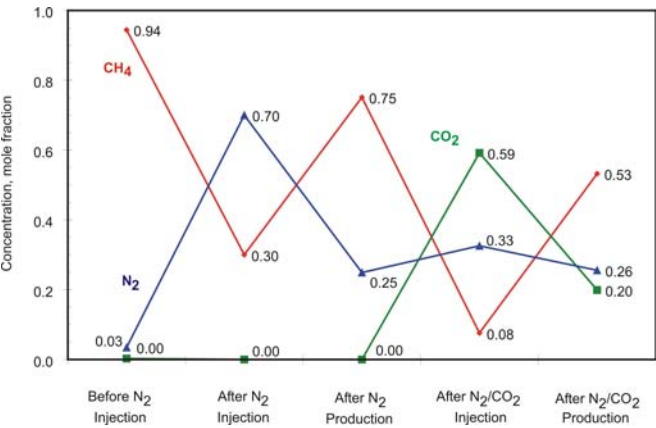


Figure 6. FBV 4A Free Gas Composition

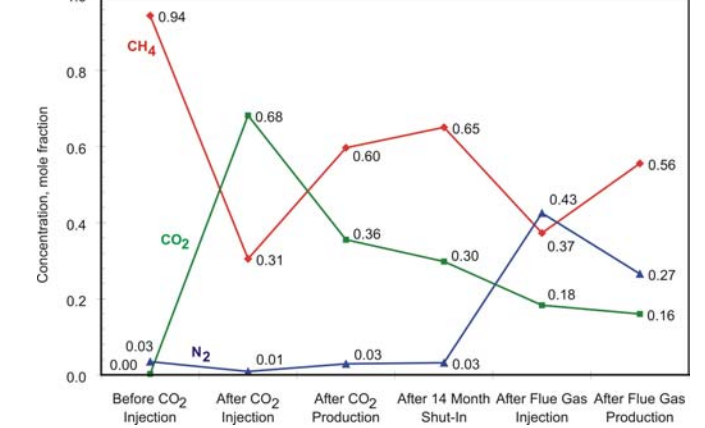


Figure 7.

FBV 5 Gas Storage Capacity

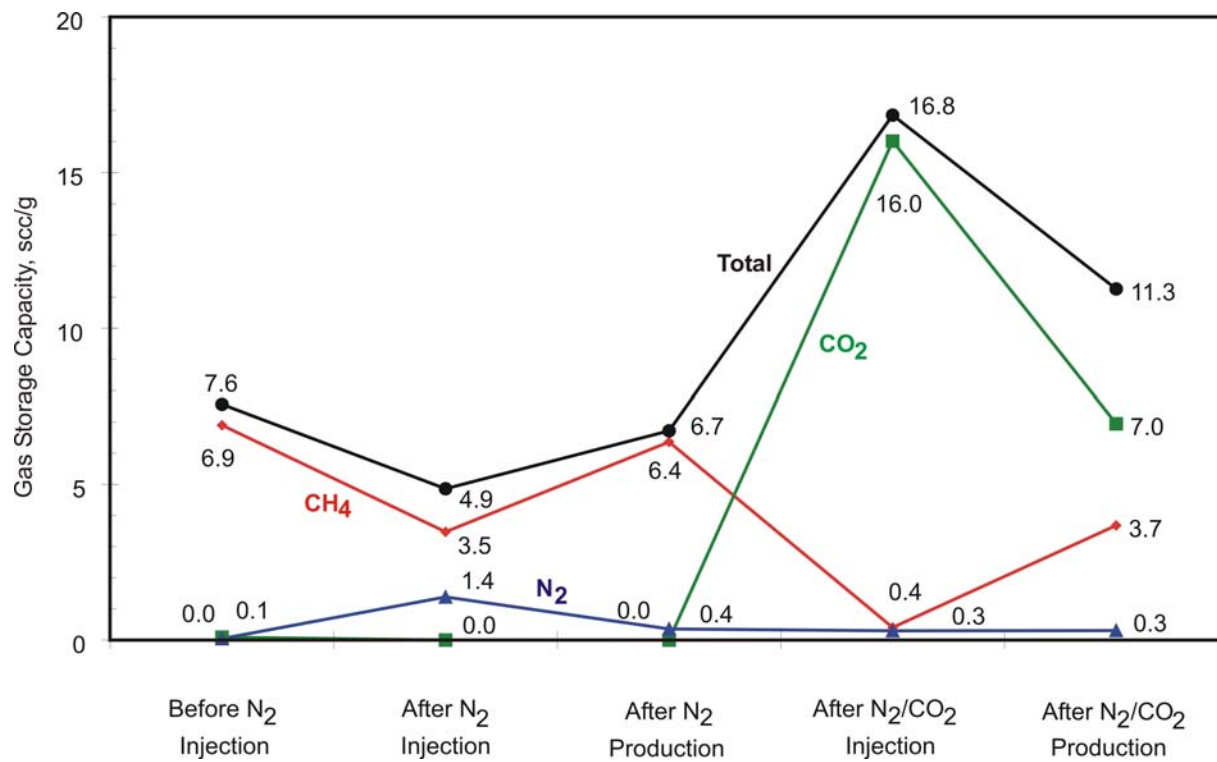


Figure 8.

FBV 4A Gas Storage Capacity

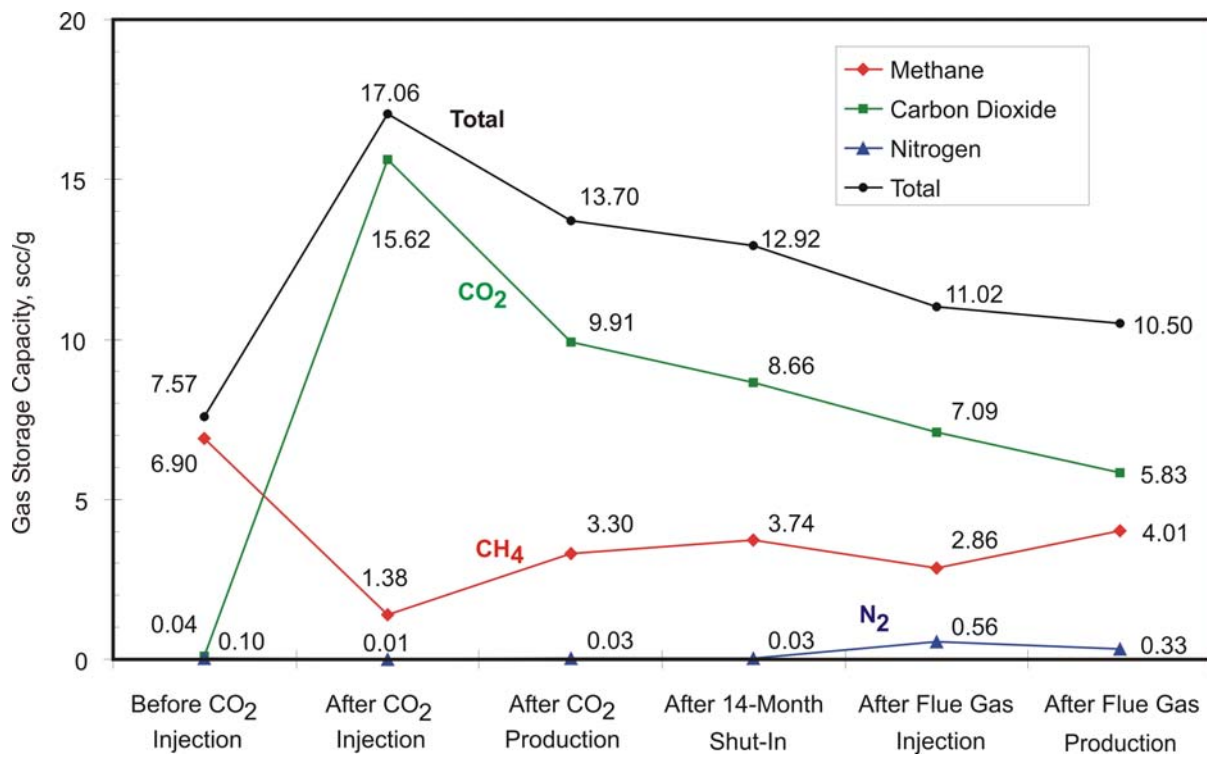


Figure 9.

### FBV 5 Gas Distribution

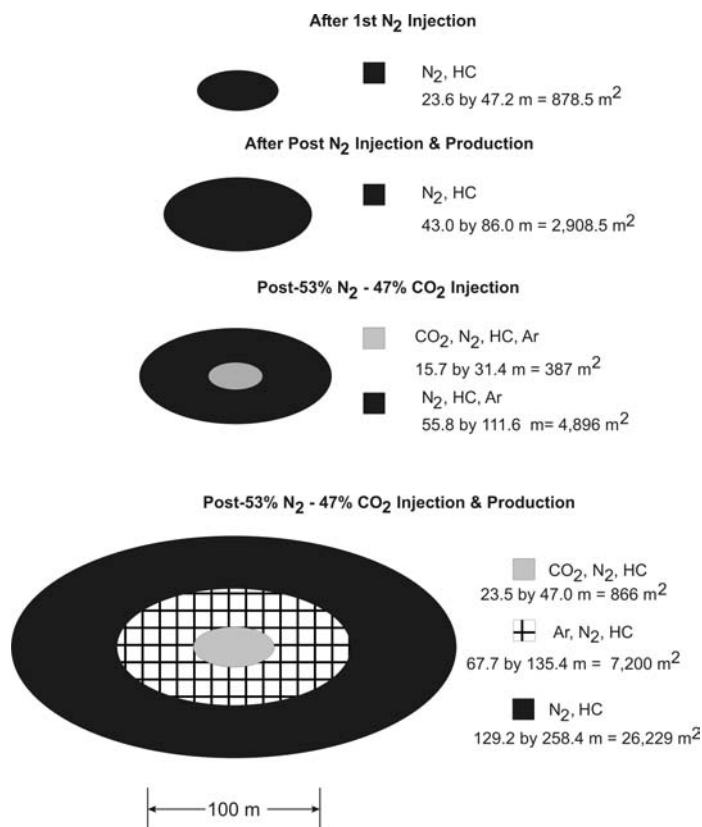


Figure 10.

### FBV 4A Gas Distribution

